



Cite this: *Mol. Syst. Des. Eng.*, 2023, 8, 942

Received 14th March 2023,  
Accepted 15th May 2023

DOI: 10.1039/d3me00042g  
[rsc.li/molecular-engineering](http://rsc.li/molecular-engineering)

## Sustainable functionalization of carbon black via dry ball milling†

Aida Kiani, Nicolas Sozio and Maria Rosaria Acocella  \*

Here, a green and sustainable functionalization of oxidized carbon black by dry ball milling with tetraphenyl phosphonium bromide (TPPBr) is reported. The reaction proceeds efficiently under solvent-free conditions, in the absence of a base, and in a reduced time with a reagent ratio of 1 to 1, much lower than the corresponding reaction in solution. The new mechanochemical approach provides the product with high stability, good mass efficiency, and high sustainability, meeting the green metrics related to waste prevention. This new procedure represents an easy way to realize new fillers and tailor their properties, such as the dispersibility in less polar environments, depending on their potential use.

### Design, System, Application

Carbon black is a widely used material in numerous industrial applications, and its chemical and physical properties can be modulated through appropriate functionalization. Mainly regarding its application as a filler in nanocomposites, achieving effective dispersion and exerting its action on the nanocomposite are significant challenges that can be addressed through appropriate surface modification. In this study, we investigate the ability of carbon black to form an ionic bond with a quaternary phosphonium salt using a dry ball milling process to provide a new type of filler with both flame retardant and antimicrobial properties. The new mechanochemical approach facilitates chemical transformations on the solid state in a solvent-free environment, representing a novel concept for achieving green chemistry and meeting environmental sustainability requirements. The process is faster, more efficient, and more cost-effective than conventional solution-based methods. Our findings demonstrate that this approach can provide new fillers to meet specific requirements, making this technique a straightforward and versatile means of generating novel materials with tailored properties.

## Introduction

Carbon black is a carbon material coming from the incomplete combustion of petroleum derivatives. It is widely used in many industrial applications, mainly as a filler in polymer matrices<sup>1–3</sup> and tires.<sup>4,5</sup> Recently considerable attention has been paid to new applications of this material in catalysis,<sup>6–10</sup> energy storage<sup>11–14</sup> and conversion,<sup>15,16</sup> renewable energy harvesting and carbon capture,<sup>17</sup> water remediation,<sup>18,19</sup> and supercapacitors.<sup>20</sup>

To make this material extensively used and applicable for different purposes, functionalization is the key step that makes it possible not only to change the polarity surface and increasing the dispersibility, but also the chemical and physical properties. So the introduction of new functional groups by the covalent or ionic bond is an important tool to have an efficient surface modification that goes before through the oxidation of carbon black. By introducing different oxygen functionalities it

is possible to further manipulate carbon materials to obtain fillers with new properties. In a previous paper, we reported for the first time the ability of oxidized carbon black (oCB) to form an ordered intercalation compound in the presence of di(hydrogenated tallow)-dimethylammonium chloride (2HT), a tetraalkylammonium cation with long hydrocarbon tails able to induce the formation of crystalline structures by self-assembling with small and disordered oCB layers.<sup>21</sup>

The ionic nature of the functionalized oCB provided by cation exchange was further confirmed by using oCB/2HT as an efficient phase transfer catalyst in an  $S_N2$  type reaction.<sup>22</sup> Recyclability and catalytic efficiency suggest that cation exchange is reversible in a suitable environment. Additionally, this functionalization changes the properties of the new filler, increasing the dispersibility of the powder in different polymer matrices. Therefore, selecting a different counterion makes it possible to control not only the features of carbon black but also those of the chosen counterion, transforming them into new ones.

In this study, carbon black is shown to bond ionically with a quaternary phosphonium salt (QPS), tetraphenyl phosphonium bromide (TPPBr), providing interesting fillers useful both as a flame retardant agent<sup>23,24</sup> and antimicrobial

Department of Chemistry and Biology "A. Zambelli", University of Salerno, Via Giovanni Paolo II, 132-84084 Fisciano, Italy. E-mail: [macocella@unisa.it](mailto:macocella@unisa.it)

† Electronic supplementary information (ESI) available. See DOI: <https://doi.org/10.1039/d3me00042g>



material.<sup>25–28</sup> In fact, the flame retardant properties of quaternary phosphonium salts were already evidenced for QPS/montmorillonite intercalated compounds, whose better dispersion in a polyamide polymer matrix guaranteed a more efficient network structure and improved flame retardant efficiency.<sup>29</sup> On the other hand, with respect to using QPS as a raw material in polymer matrices, an enhanced antimicrobial activity can be obtained as already observed using organic clays and intercalated graphite systems.<sup>25,30</sup> Mainly regarding carbon materials, graphite intercalated compounds containing phosphonium salts showed higher antimicrobial activity against *E. coli* and *S. aureus* in comparison with applying TPP directly.<sup>30</sup> Moreover, the ability of graphite oxide to provide highly ordered intercalation compounds with a quaternary phosphonium salt (QPS) was described, with an increase of crystalline order with respect to GO as well as an increase of spacing between graphite oxide layers from 0.84 to 1.40 nm, as a consequence of intercalation of the quaternary phosphonium salt. As a result of the highly ordered structure, a pH-dependent release of phosphonium ions in aqueous solutions was observed.<sup>31</sup> Based on these results, we decided to provide new fillers by using a cheaper carbon material such as carbon black choosing the QPS as a reference counterion with an easy and eco-friendly procedure not involving solvent. In fact, as previously reported,<sup>20,31</sup> the synthesis of intercalation compounds can be performed on graphite and graphene oxide as well as carbon black, using a straightforward procedure base-assisted in water solution.

An alternative, more sustainable route of functionalization is proposed here, which involves the use of mechanical grinding.

Mechanochemistry is a simple but efficient approach that enables chemical transformation by milling without dissolving reactants, thus enhancing the environmental sustainability of the process. The possibility to perform the reaction under solvent-free conditions and to modulate reaction parameters such as the material and number of balls, the reaction time, the ratio of reactants, the medium-to-sample weight ratio, and the speed of rotation allows high efficiency to be achieved.<sup>32</sup> As a matter of fact, this approach has been widely used in large-scale application production due to its low cost and simplicity.<sup>33</sup>

Recently, we reported a new eco-friendly and sustainable procedure to efficiently oxidize carbon black by using dry ball milling. As a result of the exfoliation and fragmentation of carbon materials conducted under solvent-free conditions, oxygen functionalities can be introduced into the carbon surface.<sup>34</sup> Although the degree of oxidation is comparable to that obtained by Hummers, the functional groups' nature is deeply different. Specifically, unsaturated lactones and/or ketones as well as ethers, are obtained by ball milling procedures, while epoxides, ethers, and carboxyl groups are prevalent by the Hummers method. Additionally, the surface modification of inorganic particles with polysiloxanes *via* mechanical grinding was lately reported, showing the

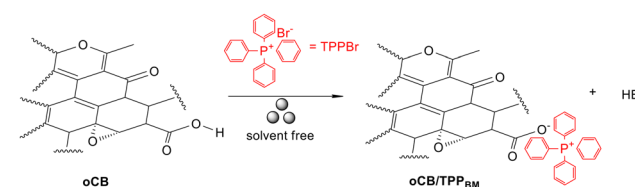
efficiency of the mechanochemical approach for surface functionalization. The reaction takes place under solvent-free conditions but requires a high molar ratio between the reagents to proceed efficiently.<sup>35</sup>

Here we show a green and sustainable functionalization of oxidized carbon black by ball milling under solvent-free conditions with tetraphenyl phosphonium bromide (TPPBr) (Scheme 1). The reaction proceeds efficiently in a very short time and with a minimum reagent ratio, affording the adduct with good reproducibility and mass production. The product can be recovered without solvent assistance, making it an eco-friendly procedure that meets most green chemistry principles. Moreover, it will be shown that mechanochemical functionalization leads to the product *via* cation exchange providing a new adduct with increased TPP dispersibility in less polar environments.

## Results and discussion

A commercial carbon black sample, exhibiting a BET surface area of  $130 \text{ m}^2 \text{ g}^{-1}$ , has been oxidized by the Hummers procedure,<sup>36</sup> chosen as the oxidation method for providing the functionalities suitable for cation exchange (alcohols, epoxy, and carboxyl groups). As evaluated by elemental analysis, the oxidized carbon black (oCB) was obtained with 0.32 as the O/C weight ratio. The oxidation step is mandatory to introduce the oxygen functionalities for further modification. As reported in FTIR (Fig. 1A), the typical vibrations between 800 and  $1300 \text{ cm}^{-1}$  due to ether, epoxy, and alcoholic groups and  $1720 \text{ cm}^{-1}$  related to carboxylic groups are evident in the spectrum of oCB as well as the degradation associated with the oxygenated functionalities in TGA (Fig. 1B). To evaluate the ability of oCB to be ionically functionalized by TPP, the reaction was performed using the procedure base-assisted previously reported in an aqueous solution<sup>20</sup> in the presence of a significant excess of the organic salt (oCB/TPP weight ratio of 1/3). After 1 h of reaction, the product needs to be extensively washed with water to remove the residual excess salt. After drying, it was recovered as a powder in 50% mass yield, as evaluated from the total amount of oCB used in the reaction.

The FTIR and TGA analyses confirm adduct formation (oCB/TPP<sub>1/3</sub>). Specifically, as shown from FTIR (Fig. 1A, blue), the peaks at 529, 694, 725, 764, 995, 1105, 1438, and  $1480 \text{ cm}^{-1}$  related to TPP are clearly observed in the adduct. As can be seen in oCB/TPP<sub>1/3</sub>, the relevant reduction in vibration associated with the carboxylic group at  $1720 \text{ cm}^{-1}$ , which is



**Scheme 1** Ionic functionalization of oCB with TPPBr promoted by ball milling under solvent-free conditions.



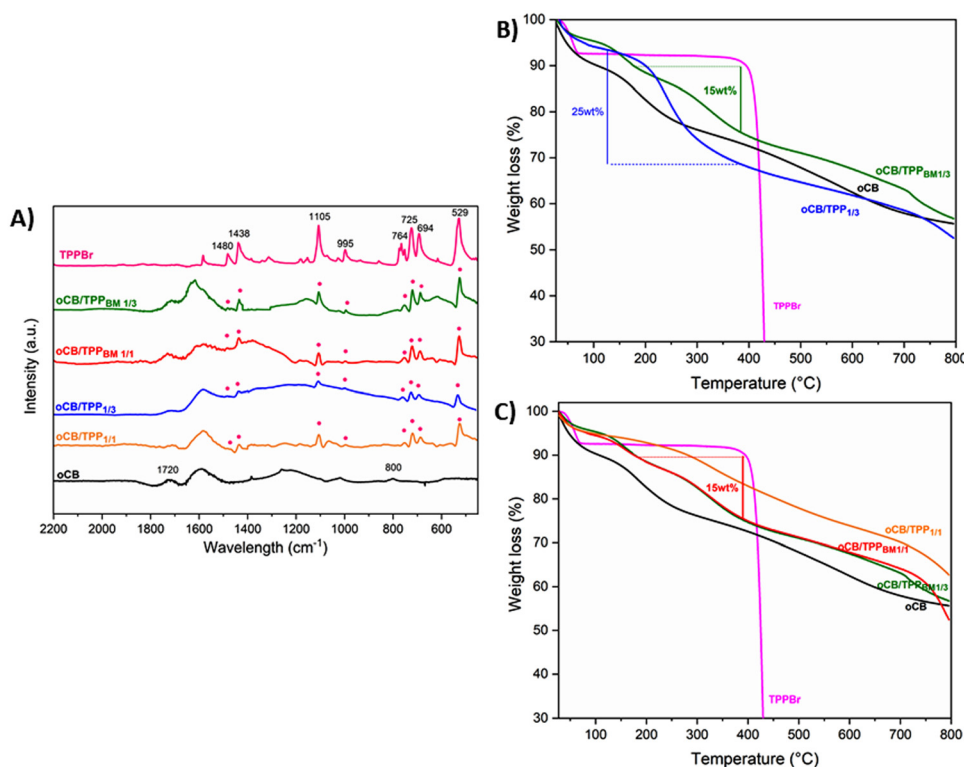


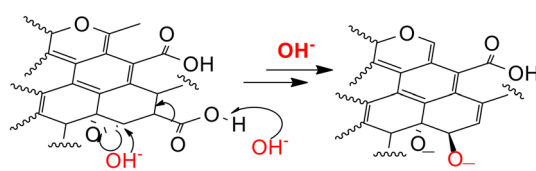
**Fig. 1** FTIR spectra (A) and TGA scans (B and C) of oCB (black), adduct oCB/TPP by reaction in solution with reagent ratios of 1/1 (orange) and 1/3 (blue), adduct oCB/TPPBM obtained by ball milling with reagent ratios of 1/1 (red) and 1/3 (green) and the TPPBr salt (pink).

evident in oCB, is possibly due to a secondary reduction reaction expected under alkaline conditions.<sup>37</sup> There is, instead, a loss of epoxide stretching at  $800\text{ cm}^{-1}$  due to the opening of the epoxy ring, which provides two nucleophilic sites for quaternary salt functionalization (see Scheme 2). Interestingly, the elemental analysis of oCB after basification and before the functionalization shows a slight reduction of the O/C ratio from 0.32 of the starting oCB to 0.30 after basification according to the possible mechanism shown in Scheme 2.

Moreover, the occurrence of the cation exchange was further proved by TGA analysis (Fig. 1B). A comparison of the adduct with the starting oCB and TPPBr shows that oCB/TPP<sub>1/3</sub>, as obtained by the solution, presents a decomposition above  $200\text{ }^\circ\text{C}$  and a TPP content close to 25 wt% also confirmed by elemental analysis (see ESI†).

The X-ray diffraction pattern of oCB/TPP<sub>1/3</sub> is shown in Fig. 2, and only the broad diffraction halo of oCB can be

detected. Furthermore, the complete loss of TPP crystallinity clearly demonstrates the adduct formation and absence of the residual unreacted salt on the powder surface. As with graphite oxide, it might be assumed that carbon black can provide intercalation compounds, but being characterized by a disordered spatial arrangement, no structural order can be detected in the X-ray diffraction pattern. More interestingly is the relative instability of oCB/TPP<sub>1/3</sub> after 30 days of storage at room temperature and humidity range of 50–70%, as



**Scheme 2** Proposed mechanism of decarboxylation and epoxy ring opening in alkaline solution.

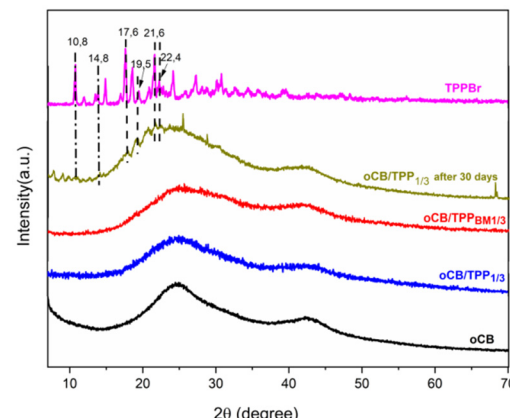


**Fig. 2** X-ray diffraction patterns of oCB (black), oCB/TPP<sub>1/3</sub> (blue) as obtained in solution, oCB/TPP<sub>BM</sub> 1/3 as obtained by ball milling (red), oCB/TPP<sub>1/3</sub> after 30 days (olive), and TPPBr salt (pink).

observed by X-ray diffraction pattern. As from Fig. 2, many newly defined peaks are present after 30 days with respect to oCB/TPP<sub>1/3</sub> as freshly prepared, attributing some of them to TPPBr ( $2\theta = 10.8^\circ, 14.8^\circ, 17.6^\circ, 19.5^\circ, 21.6$ , and  $22.4^\circ$ ).

After extensively washing in water solution, the new reflections disappear in the X-ray diffraction pattern as well as the vibrations corresponding to the salt in the FTIR spectrum (Fig. 3A). Moreover, the TGA degradation clearly shows a substantial reduction of salt uptake after washing (Fig. 3B). This behavior is possibly due to the evolution of basified oCB in a more thermodynamically stable system with restoring the aromatic structure as previously reported in precedent papers<sup>37,38</sup> and the formation of free salts easily removed by water solution (see ESI†).

### Solvent-free mechanical functionalization

An alternative, more sustainable route of functionalization of oCB is mechanical grinding, which, operating under solvent-free conditions, simplifies the process considerably. The reaction was performed by using an 80 ml jar and 8 balls with a diameter of 10 mm, both in silicon nitride. The reaction was carried out in the presence of 200 mg reagent considering the reaction conditions already used in solution with a relative ratio between oCB and TPPBr of 1 to 3 and at a rotational speed of 300 rpm. NaOH was missing in the mechanochemical procedure to avoid a fast reduction pathway of oCB under alkaline conditions due to the solvent-free conditions.

Surprisingly, the reaction not only proceeds in 30 minutes but also affords the functionalized adduct oCB/TPP<sub>BM1/3</sub> in 64% mass yield, higher than the corresponding product provided by the reaction in solution. The FTIR and TGA analyses both confirm the adduct formation. Specifically, as shown from FTIR (Fig. 1A), the peaks at 529, 694, 725, 764, 995, 1105, 1438, and 1480  $\text{cm}^{-1}$  related to TPP are clearly observed in oCB/TPP<sub>BM1/3</sub>.

TGA analysis further proved the adduct formation (Fig. 1B, green curve). A comparison of the adduct with the

starting oCB and TPPBr shows that the oCB/TPP<sub>BM1/3</sub>, obtained by ball milling, presents a TPP content close to 15 wt%.

The reduced uptake observed in oCB/TPP<sub>BM1/3</sub> could be explained based on the different mechanisms of functionalization occurring in the absence of a base. While in solution the presence of a base assures epoxy opening with the consequent formation of two new anionic sites and an increase of the salt uptake (see Scheme 2), in the ball milling procedure, the fast ionic exchange could preferentially occur with the more acidic proton of the carboxylic group that appears to be the same after grinding (oCB/TPP<sub>BM1/3</sub> vs. oCB, Fig. 1A).

The X-ray diffraction pattern of oCB/TPP<sub>BM1/3</sub> is shown in Fig. 2, and only the broad diffraction halo of oCB can be detected. Furthermore, the complete loss of TPP crystallinity clearly demonstrates the adduct formation and absence of the residual unreacted salt on the powder surface.

It is worth noting that, unlike the adduct obtained by the reaction in solution, oCB/TPP<sub>BM1/3</sub> shows high stability even after 30 days, as from its X-ray diffraction pattern superimposable with the fresh one reported in Fig. 2. In the attempt to improve the procedure, a reduction of milling time to 5 minutes was tested on our reaction system, providing the same adduct but with less efficiency (uptake less than 10%), while extending the milling time did not increase the uptake and mass yield.

An interesting finding was the result obtained by reducing the weight ratio between the reagents. Specifically, the reaction was performed using oCB and TPPBr in a ratio of 1 to 1 with 30 minutes of milling time.

Surprisingly, the adduct was obtained with the same salt uptake of the 1 to 3 mixture as observed from FTIR and TGA (oCB/TPP<sub>BM1/1</sub> (red) *versus* oCB/TPP<sub>BM1/3</sub> (green) Fig. 1A and C), but with a higher mass yield (up to 80%).

No significant changes were detected in the X-ray diffraction pattern that shows again the complete loss of TPP crystallinity, clearly demonstrating the adduct formation. For the sake of comparison, the reaction in the presence of the

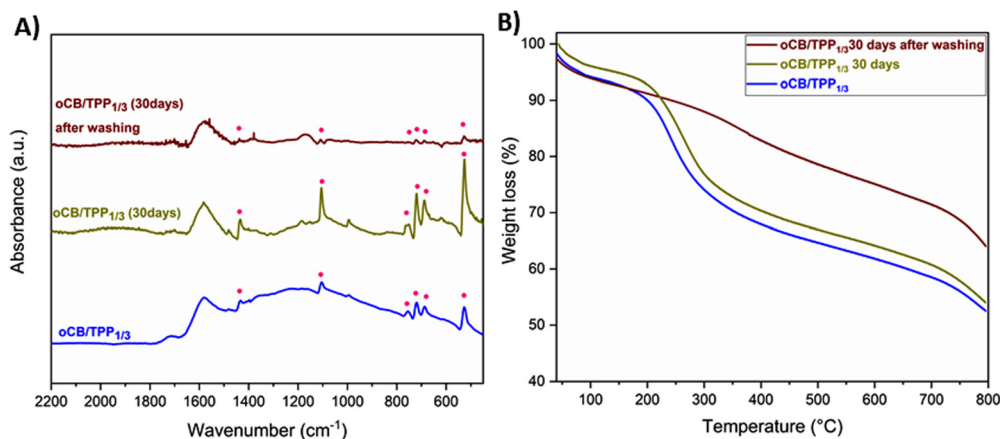


Fig. 3 FTIR spectra (A) and TGA scans (B) of oCB/TPP<sub>1/3</sub> (blue), oCB/TPP<sub>1/3</sub> after 30 days (green), and oCB/TPP<sub>1/3</sub> after 30 days and after washing (brown).



same reagent ratio was performed in an alkaline solution. As for FTIR and TGA (Fig. 1A and C), the adduct oCB/TPP<sub>1/1</sub> can be obtained in solution but with reduced efficiency with respect to the reaction performed by ball milling under the same conditions.

To better optimize the process conditions, the chemical nature of the balls and the speed rate were changed. The reaction performed in the presence of tempered steel results in a decreased functionalization possibly due to the stronger collisions that reduced the carboxyl functionalities as clearly observed by FTIR analysis (see ESI†). Additionally, the reaction was carried out at 100 and 500 rpm to explore the influence of the speed rate on the functionalization degree. It was determined that a reduced speed of 100 rpm provides a lower functionalization requiring a longer time to reach the same as for 300 rpm, while an increased speed of up to 500 rpm had no positive impact on the reaction. As a result, 300 rpm was found to be the best compromise between the reaction time and functionalization degree. Further evaluation of the feeding amount showed an increase in mass yield of up to 99% in the presence of a 500 mg reagent mixture.

To confirm the ionic nature of the adduct, an additional test was performed by using oxidized carbon black obtained by ball milling oxidation, which is characterized by the presence of unsaturated ketones and lactones and the absence of carboxyl groups.<sup>34</sup>

The reaction was carried out under the optimized conditions, but no functionalization occurred showing the necessary contribution of the carboxyl group to promote the ionic exchange.

A pH-sensitive cation release further verified the ionic nature of the adduct obtained by ball milling. In particular, neutral (pH = 7 with 10 wt% NaCl) and acid (pH = 1.3, HCl 0.05 M) solutions have been considered comparing the kinetic release of TPP during that time.

The amount of TPP<sup>+</sup> was evaluated by UV measurement in the spectral range 250–350 nm in the aqueous solution. Specifically, the UV spectra obtained after 5 h of soaking time are compared in Fig. 4A and clearly show the ability of TPP<sup>+</sup> to be released under acidic conditions.

As can be seen from Fig. 4B, the release of TPP<sup>+</sup> ions in the aqueous acidic solution is complete already after 3 h. In comparison, only a negligible release can be detected under neutral conditions even after 5 h because of the limited cation exchange promoted under these conditions.

Additionally, ionic functionalization alters the ability of TPP to disperse in different media, making oCB/TPP the right method for conveying TPP in less polar environments, such as different polymer matrices, without aggregation. Hence, dispersibility tests were performed in water, acetonitrile, and ethyl acetate, chosen as solvents with different polarity indexes, for the TPPBr and the adduct oCB/TPP, respectively.

As a result of its ionic nature, TPPBr shows high solubility in polar solvents, protic and non-protic such as H<sub>2</sub>O and CH<sub>3</sub>-CN. However, a very poor solubility has been observed by decreasing the polarity of the solvent, such as in ethyl acetate. As can be seen from Fig. 5, the suspension of TPP in ethyl acetate shows consistent white sediment (Fig. 5, inset A).

Conversely, it is clear after functionalization that not only does the oCB/TPP powder disperse in polar media, but also in less polar solvents such as ethyl acetate, as shown in Fig. 5 inset B.

### Green metrics

The procedure described shows the ability of ball milling to provide carbon functionalization through an eco-friendly process reducing the amount of reagent, reaction time and working under solvent-free conditions, meeting the first principle of green chemistry related to waste prevention. To further show the high quality and environmental sustainability

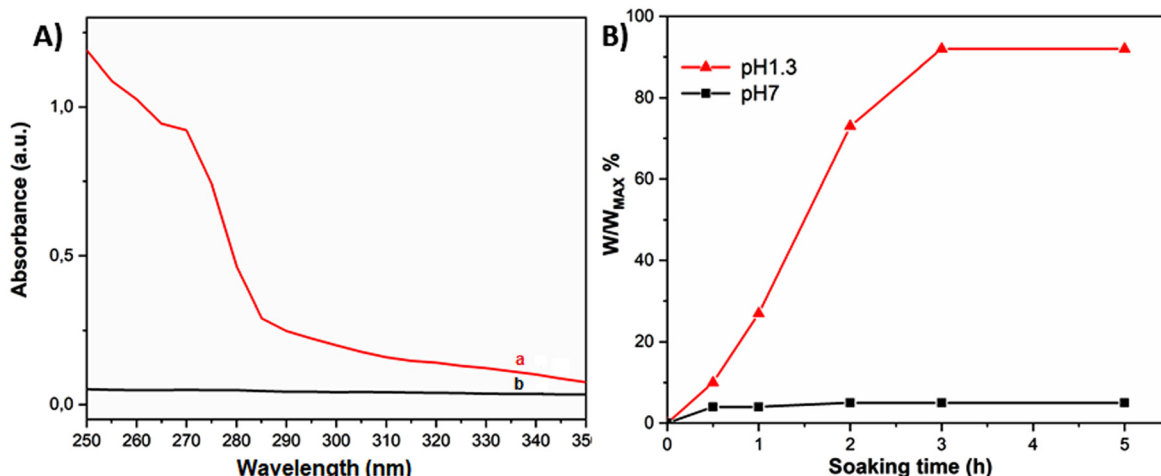
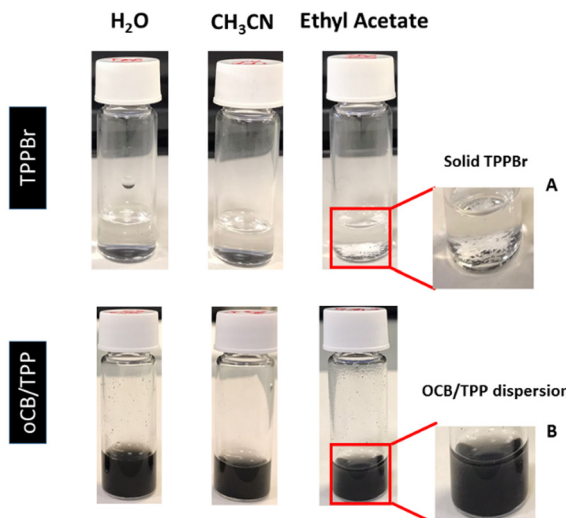


Fig. 4 (A) UV measurements in the spectral range 250–350 nm, in the neutral aqueous solution (b) and acidic solution (a) after 5 h of soaking time; (B) TPP<sup>+</sup> kinetic release from oCB/TPP<sub>BM1/1</sub> in neutral saline solution (pH = 7 black curve, squares) and in acidic solution (pH = 1.3, red curve, triangles) expressed as a percentage of the long term release.





**Fig. 5** TPPBr and oCB/TPP in water, acetonitrile, and ethyl acetate solution 5 mg mL<sup>-1</sup>, after 5 min of sonication and 30 minutes of storage. Inset A and B: solid TPPBr as sediment and oCB/TPP dispersion in ethyl acetate, respectively.

of this procedure, a comparison of the two different routes, in solution and *via* ball milling under the best reaction conditions (reagent ratio of 1/3 and 1/1 for solution and ball milling synthesis, respectively), should be done taking into account some of the most important green metrics such as atom efficiency (AE), environmental factor (E factor), process mass intensity (PMI), mass productivity (MP) and Ecoscale. The AE and E factor are the most popular green metrics that allow us to predict and evaluate, respectively, the amount of waste that will be generated.<sup>39</sup> Alternative mass-based metrics have been used for assessing the sustainability of the process as PMI and MP, both focusing on optimizing resource utilization (Fig. 6). Specifically, a lower PMI and a higher MP result in less waste production.

An interesting tool for selecting the best synthetic route based on economic and ecological parameters is the Ecoscale. This approach is based on assigning a range of penalty points on a starting score of 100, depending on the yield, price of reagents, safety, technical setup, temperature/time, workup, and purification.<sup>40</sup> The higher the Ecoscale, the higher the sustainability.

As reported in Table 1, the greater efficiency of the ball milling approach with respect to the solution reaction in terms of green metrics is evident. Although the AE was evaluated on the fresh products, without considering the products' instability deriving from the reaction in solution in the first weeks after the synthesis, all the parameters are

$$AE = \frac{\text{mol wt of product}}{\text{sum of mol wts of reactants}} * 100$$

$$E = \frac{\text{Total mass waste}}{\text{Mass of product}}$$

$$PMI = \frac{\text{Total mass in process (incl water)}}{\text{Mass of product}}$$

$$MP = \frac{\text{Mass of product}}{\text{Total mass (incl solvents)}} * 100$$

**Fig. 6** Green metrics for the eco-friendly process.

**Table 1** Comparison of green metrics for oCB/TPP<sub>1/3</sub> in solution and oCB/TPP<sub>BM1/1</sub> by ball milling

Green metrics	oCB/TPP <sub>1/3</sub>	oCB/TPP <sub>BM1/1</sub>
AE	78 <sup>a</sup>	83
E factor	2.7 <sup>b</sup>	0
PMI	10.7	2.5
MP	9	40
Ecoscale <sup>c</sup>	75	90

<sup>a</sup> The AE was evaluated on the fresh product without considering the instability responsible for side products. <sup>b</sup> The E factor was evaluated by looking at alkaline water as waste. <sup>c</sup> The Ecoscale value was evaluated based on the classification reported in ref. 38.

considerably better for the reaction with ball milling (to know more details about the calculations, see the ESI†).

Specifically, while ball milling enables the reaction to proceed under dry conditions without waste production, the reaction in solution produces alkaline water as waste, providing an E factor of 2.7.

Moreover, both the PMI and MP are lower and higher, respectively, for the ball milling procedure where the best reagent ratio is 1/1, resulting in higher efficiency and less waste production.

More interestingly is the Ecoscale comparison between the two procedures, which once again rewards the ball milling approach because of the higher mass efficiency observed, confirming the increased sustainability of our procedure.

## Experimental section and methods

### Materials

Carbon black samples (CB) of grade N110 containing 99.8% carbon and a BET surface area of 130 m<sup>2</sup> g<sup>-1</sup> were purchased from Cabot Company (USA). Sulfuric acid, sodium nitrate, potassium permanganate, and tetraphenylphosphonium bromide (TPPBr) were purchased from Sigma-Aldrich. All reagents were used as received without purification.

### Oxidation of carbon black

In a 1000 mL three-neck, round-bottomed flask immersed in an ice bath, 12 mL sulfuric acid and 0.25 g sodium nitrate were combined with 0.5 g of carbon samples. A uniform dispersion was obtained before adding 1.5 grams of potassium permanganate very slowly to minimize explosion risks. The black and dark green slurry of carbon black was added to small amounts of deionized water (70 mL), stirred, and then 0.5 mL of H<sub>2</sub>O<sub>2</sub> (30 wt%). A Neya16 centrifuge was used to separate the sample from the water solution at 8500 rpm for 15 minutes using 700 mL of deionized water. The oCB powders were first washed twice with 10 mL of a 5 wt% HCl aqueous solution and subsequently washed with 50 mL of deionized water. Finally, powders were dried at 60 °C for 12 h. About 0.4 g of oCB sample was obtained.

## Preparation of oCB/TPP<sub>1/1</sub> and oCB/TPP<sub>1/3</sub> intercalation compounds in solution

In this study, intercalation with TPP<sup>+</sup> was performed according to the procedure reported in ref. 20. oCB powders (50 mg) were dispersed in 0.05 M NaOH solution (10 mL), a TPPBr solution (50 mg or 150 mg TPPBr (according to the ratio) in (50 mL) deionized water) was added in this dispersion, and the reaction mixture was stirred at room temperature for 1 h. The slurry was centrifuged at 10 000 rpm for 15 min, and the precipitate was washed with deionized water and dried at 60 °C for 12 h in an oven.

## Preparation of oCB/TPP<sub>BM1/1</sub> and oCB/TPP<sub>BM1/3</sub> intercalation compounds via ball milling

The ball-milling experiments were conducted at room temperature in a planetary ball mill Pulverisette 7 Premium (Fritsch GmbH, Germany). Samples were labelled oCB/TPP<sub>BM1/1</sub> and oCB/TPP<sub>BM1/3</sub> according to the ratio between oCB and TPPBr respectively. 50 mg of oCB powders and 50 mg TPPBr for oCB/TPP<sub>BM1/1</sub>, or 150 mg TPPBr in the case of oCB/TPP<sub>BM1/3</sub> were added directly in an 80 ml silicon nitride jar. The milling parameters were set as shown in Table S1 of the ESI.† Silicon nitride balls with a diameter of 10 mm were used in all procedures. The rotational frequency was examined at 300 rpm and for 30 minutes. The 5-minute break was taken every 5 minutes before the milling resumed. In order to determine the mass yield of the milled product, samples were weighed after ball milling. An Easy-GTM system (Fritsch GmbH, Germany) was used to measure the temperature of the milling beakers.

## Characterization

FTIR spectra were obtained at a resolution of 2.0 cm<sup>-1</sup> with an FTIR (BRUKER Vertex 70) spectrometer equipped with a deuterated triglycine sulfate (DTGS) detector and a KBr beam splitter using KBr pellets. The frequency scale was internally calibrated to 0.01 cm<sup>-1</sup> using a He-Ne laser. The noise was reduced by signal-averaging 32 scans.

Wide-angle X-ray diffraction (WAXD) patterns were obtained using an automatic Bruker D2 phaser diffractometer, in reflection, at 35 KV and 40 mA, using nickel-filtered Cu K $\alpha$  radiation (1.5418 Å).

The thermogravimetric analysis (TGA) was performed on a Q500 TA Instruments, from 10 to 800 °C at a heating rate of 10 °C, under N<sub>2</sub>. Weight decreases below 100 °C were used to determine the water content.

Elemental analysis was performed with a Thermo FlashEA 1112 Series CHNS-O analyzer.

UV-vis spectra were recorded using a PerkinElmer Lambda 800 UV-vis spectrophotometer.

## Conclusions

A green and sustainable functionalization of oxidized carbon black by ball milling under solvent-free conditions with

tetraphenyl phosphonium bromide (TPPBr) has been reported here for the first time, providing a new filler useful both as a flame-retardant agent and antimicrobial material.

The reaction proceeds efficiently under solvent-free conditions, without the assistance of a base, in reduced time affording the adduct with higher stability and mass production than the corresponding reaction in solution.

Moreover, the same functionalization can be achieved with a reagent ratio of 1 to 1, much lower than the corresponding reaction in solution, with higher mass efficiency meeting the first principle of green chemistry related to waste prevention.

The adducts can be recovered without solvent assistance, making it an environmentally friendly procedure that meets most green chemistry metrics.

Furthermore, the mechanochemical functionalization provides the adduct *via* cation exchange and improves the ability of TPP to disperse in less polar environments, for example, polymer matrices with reduced polarity. This new procedure, therefore, represents a very straightforward way to develop new fillers and, appropriately choosing the counterion, customize their properties according to the intended application.

Further studies are currently in progress to evaluate the influence of the counterion on the mechanical and physiochemical properties of different polymer matrices.

## Author contributions

Aida Kiani: methodology, software, validation, visualization, investigation, data curation, formal analysis, validation. Nicolas Sozio: methodology, software, formal analysis. Maria Rosaria Acocella: conceptualization, visualization, supervision, writing – original draft, writing – review & editing.

## Conflicts of interest

There are no conflicts to declare.

## Acknowledgements

Financial support from “Ministero dell’Università e della Ricerca” is gratefully acknowledged.

## References

1. S. Xu, M. Wen, J. Li, S. Guo, M. Wang, Q. Du, J. Shen, Y. Zhang and S. Jiang, *Polymer*, 2008, **49**, 4861.
2. L. D’Urso, M. Acocella, G. Guerra, V. Iozzino, F. De Santis and R. Pantani, *Polymer*, 2018, **10**, 139.
3. L. D’Urso, M. R. Acocella, F. De Santis, G. Guerra and R. Pantani, *Polymer*, 2022, **256**, 125237.
4. Y. Fan, G. D. Fowler and M. Zhao, *J. Cleaner Prod.*, 2020, **247**, 119115.
5. L. B. Tunnicliffe and J. J. C. Busfield, *Designing of Elastomer Nanocomposites: From Theory to Applications*, ed. K. W. Stöckelhuber, A. Das and M. Klüppel, Springer International Publishing, Cham, 2017, p. 71.



6 M. R. Acocella and G. Guerra, *ChemCatChem*, 2018, **10**, 2350.

7 C. Su and K. P. Loh, *Acc. Chem. Res.*, 2013, **46**, 2275.

8 M. R. Acocella, A. Vittore, M. Maggio, G. Guerra, L. Giannini and L. Tadiello, *Polymer*, 2019, **11**, 1330.

9 M. R. Acocella, M. Maggio, C. Ambrosio, N. Aprea and G. Guerra, *ACS Omega*, 2017, **2**, 7862.

10 R. Villano, M. R. Acocella and G. Guerra, *ChemistrySelect*, 2017, **2**, 10559.

11 C. Liu, X. Liu, J. Tan, Q. Wang, H. Wen and C. Zhang, *J. Power Sources*, 2017, **342**, 157.

12 Y. Zhou, L. Liu, Y. Shen, L. Wu, L. Yu, F. Liang and J. Xi, *Chem. Commun.*, 2017, **53**, 7565.

13 S. Liang, C. Liang, Y. Xia, H. Xu, H. Huang, X. Tao, Y. Gan and W. Zhang, *J. Power Sources*, 2016, **306**, 200.

14 M. Oschatz, S. Thieme, L. Borchardt, R. M. Lohe, T. Biemelt, J. Brückner, H. Althues and S. Kaskel, *Chem. Commun.*, 2013, **49**, 5832.

15 S. Zhuang, E. S. Lee, L. Lei, B. B. Nunna, L. Kuang and W. Zhang, *Int. J. Energy Res.*, 2016, **40**, 2136.

16 G. Wang, J. Zhang and S. Hou, *Mater. Res. Bull.*, 2016, **76**, 454.

17 S. Khodabakhshi, Pa. F. Fulvio and E. Andreoli, *Carbon*, 2020, **162**, 604.

18 X. Cao, S. Sun and R. Sun, *RSC Adv.*, 2017, **7**, 48793.

19 Y. Huang, J. Tang, L. Gai, Y. Gong, H. Guan, R. He and H. Lyu, *Chem. Eng. J.*, 2017, **319**, 229.

20 C. Schneidermann, N. Jäckel, S. Oswald, L. Giebel, V. Presser and L. Borchardt, *ChemSusChem*, 2017, **10**, 2416–2424.

21 M. Maggio, M. Rosaria Acocella and G. Guerra, *RSC Adv.*, 2016, **6**, 105565.

22 A. Melillo, A. Kiani, R. Schettini and M. R. Acocella, *Mol. Catal.*, 2023, **537**, 112951.

23 W.-T. He, S.-T. Liao, Y.-S. Xiang, L.-J. Long, S.-H. Qin and J. Yu, *Polymer*, 2018, **10**, 312.

24 S. V. Levchik and E. D. Weil, *J. Fire Sci.*, 2006, **24**, 345.

25 P. Herrera, R. C. Burghardt and T. D. Phillips, *Vet. Microbiol.*, 2000, **74**, 259.

26 A. Xie, W. Yan, X. Zeng, G. Dai, S. Tan, X. Cai and T. Wu, *Bull. Korean Chem. Soc.*, 2011, **32**, 1936.

27 X. Cai, S. Tan, M. Liao, T. Wu, R. Liu and B. Yu, *J. Cent. South Univ. Technol.*, 2010, **17**, 485.

28 W. Tan, J. Zhang, F. Luan, L. Wei, Y. Chen, F. Dong, Q. Li and Z. Guo, *Int. J. Biol. Macromol.*, 2017, **102**, 704.

29 W.-T. He, S.-T. Liao, Y.-S. Xiang, L.-J. Long, S.-H. Qin and J. Yu, *Polymer*, 2018, **10**, 31.

30 A.-G. Xie, X. Cai, M.-S. Lin, T. Wu, X. J. Zhang, A.-D. Lin and S. Tan, *Mater. Sci. Eng., B*, 2011, **176**, 1222.

31 M. Mauro, M. Maggio, A. Antonelli, M. R. Acocella and G. Guerra, *Chem. Mater.*, 2015, **27**, 1590.

32 J.-L. Do and T. Friščić, *ACS Cent. Sci.*, 2017, **3**, 13.

33 Y. Yao, Z. Lin, Z. Li, X. Song, K.-S. Moon and C. Wong, *J. Mater. Chem.*, 2012, **22**, 13494.

34 A. Kiani, M. R. Acocella, V. Granata, E. Mazzotta, C. Malitesta and G. Guerra, *ACS Sustainable Chem. Eng.*, 2022, **10**, 16019.

35 H. Kim, J. E. Lee, S.-M. Jo and S. Wooh, *ACS Sustainable Chem. Eng.*, 2022, **10**, 9679.

36 W. S. Hummers and R. E. Offeman, *J. Am. Chem. Soc.*, 1958, **80**, 1339.

37 E. Cascone, S. Longo and M. R. Acocella, *ACS Omega*, 2022, **7**, 25394.

38 A. M. Dimiev, L. B. Alemany and J. M. Tour, *ACS Nano*, 2013, **7**, 576.

39 R. A. Sheldon, *ACS Sustainable Chem. Eng.*, 2018, **6**, 32.

40 K. V. Aken, L. Strelkowski and L. Patiny, *Beilstein J. Org. Chem.*, 2006, **2**, 3.

